Deep-Sea Research Part II 169-170 (2019) 104605

Contents lists available at ScienceDirect

Deep-Sea Research Part II

journal homepage: www.elsevier.com/locate/dsr2

Variations in black-footed albatross sightings in a North Pacific transitional area due to changes in fleet dynamics and oceanography 2006–2017.

Johanna L.K. Wren[a,b,*], Scott A. Shaffer[c], Jeffrey J. Polovina[b]

[a] Joint Institute for Marine and Atmospheric Research, Wasp Blvd., bldg. 176, Honolulu, Hawai'i, 96818, USA
[b] Pacific Islands Fisheries Science Center, Wasp Blvd., bldg. 176, Honolulu, Hawai'i, 96818, USA
[c] Department of Biological Sciences, San José State University, San Jose, CA, 95192, USA

ARTICLE INFO

Keywords:
Transitional area
Black-footed albatross
Pacific decadal oscillation
Fisheries interactions
Hawai'i-based longline fishery
Phoebastria nigripes

ABSTRACT

A serious threat to pelagic seabird populations today is interactions with longline fisheries. While current seabird mitigation efforts have proven successful in substantially reducing seabird interactions in the Hawai'i-based longline fishery, black-footed albatross (*Phoebastria nigripes*) interactions have increased. In an effort to better understand when and where these interactions take place, we explore the relationship between black-footed albatross sightings in the Hawai'i-based deep-set longline fishery and fleet dynamics and environmental variables. Environmental drivers include both large scale climate variability due to the Pacific Decadal Oscillation (PDO) and El Niño – Southern Oscillation, as well as local oceanographic and atmospheric drivers, such as wind patterns, sea surface temperature, and surface chlorophyll. Using generalized linear models, we found that while season, latitude, and longitude of fishing explained much of the variation throughout the time series, both large scale and local climate variables – positive PDO, strong westerly winds, and sea surface temperature fronts – explained the increase in black-footed albatross sightings in recent years. Black-footed albatross nest in the Northwestern Hawaiian Islands, and their main foraging habitat while nesting are the productive fronts to the north and east of the Hawaiian Islands. During a positive PDO, a more intense and expanded Aleutian Low shifts westerly winds southward, replacing trade winds in the northern region of the longline fishing grounds. The expanded westerly winds may have two impacts. Firstly, they drive productive surface waters to the south, increasing the overlap of the albatross foraging grounds and the deep-set fishing grounds. Secondly, when westerlies move south, more birds transit through the fishing grounds to the east rather than traveling north to reach the westerlies before traveling eastward north of the fishing grounds. Because PDO operates on decadal timescales, the high levels of sightings and interactions may persist for many years.

1. Introduction

One of the greatest threats to pelagic seabird populations today is interactions with longline fisheries (Bakker et al., 2018; Lewison and Crowder, 2003; Tuck et al., 2001). The deep-set Hawai'i-based longline fishery targets bigeye tuna (*Thunnus obesus*); however, incidental catch of commercially valuable fish and vulnerable marine mammals, sea turtles, and seabirds occurs. Occasionally, seabirds seize and engulf baited hooks as they are set, get hooked and/or entangled, get pulled underwater, and are drown as the gear sinks. In an effort to protect seabird populations and reduce interactions, the Hawai'i longline fishery adopted mitigation methods in 2001, with a recent amendment to the methods in 2006 (Pacific Islands Regional Office, 2018a).

Because the majority (90%) of seabirds are caught to the north of the main Hawaiian Islands, when fishing north of 23°N all deep-set longline vessels must use one of two suites of seabird mitigation methods: side setting or blue-dyed bait (Pacific Islands Regional Office, 2018a). Side setting includes setting gear off the side of a vessel instead of the stern, with the mainline as far forward as possible but no less than 1 m from the stern; deploying a bird curtain; using a minimum of 45 g weights attached < 1m from the hook on branch lines; and gear must be deployed so that baited hooks stay submerged. The blue-dyed bait method includes strategic discard of bait or offal from the opposite side of where the gear is being hauled or set; thawing the bait and dying it blue; using a minimum of 45 g weights attached < 1m from the hook on branch lines; and using a mainline shooter (National Oceanic and Atmospheric Administration (NOAA), National Marine Fisheries Service (NMFS), 2005). While these efforts to reduce seabird bycatch have been successful – with a 67% decrease in interactions since mitigation methods were instituted (Gilman et al., 2016, 2008) – black-footed

* Corresponding author. Joint Institute for Marine and Atmospheric Research, Wasp Blvd., bldg. 176, Honolulu, Hawai'i, 96818. USA.
E-mail address: johanna.wren@noaa.gov (J.L.K. Wren).

https://doi.org/10.1016/j.dsr2.2019.06.013
Received 15 October 2018; Received in revised form 1 May 2019; Accepted 20 June 2019
Available online 22 June 2019

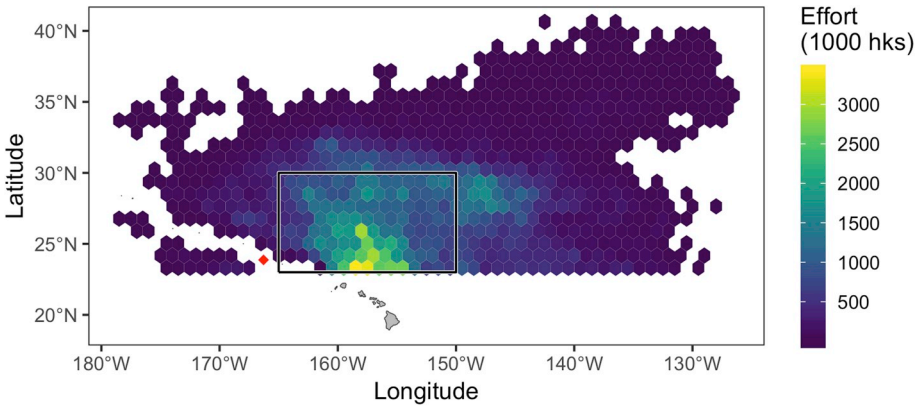

Fig. 1. Map of the Hawai'i longline fishing grounds (gray box) with total observed effort in 1000 hooks for 2006–2017 in color summarized in 5-degree hexagons. The black box outlines the area of high effort, and this is the area we used as the "high interaction area" for black-footed albatross (*Phoebastria nigripes*). The red diamond to the left of the box marks Tern Island. (For interpretation of the references to color in this figure legend, the reader is referred to the Web version of this article.)

albatross (*Phoebastria nigripes*) interactions in the Hawai'i-based deep-set longline fishery have increased more than threefold in 2015–2017, compared with the preceding ten years (Gilman et al., 2016; Pacific Islands Regional Office, 2018a) (Fig. 1). Laysan albatross (*Phoebastria immutabilis*) are also caught in the Hawai'i-based longline fishery but the interaction rates are lower than that for black-footed albatross and have remained steady since the implementation of mitigation methods (Pacific Islands Regional Office, 2018a), likely due to Laysan habitat use north and west of the breeding colonies and outside of the longline fishing grounds (Antolos et al., 2017; Thorne et al., 2016, 2015)(Fig. 1). Our focus in this study is on black-footed albatross.

Black-footed albatrosses are long-lived marine birds with large foraging habitats (Hyrenbach et al., 2002; Kappes et al., 2015, 2010) and low annual reproductive rates (Tickell, 2000; Warham, 1990). Their oceanic habitat spans most of the north Pacific Ocean, but the majority (95%) of the birds nest in the Northwestern Hawaiian Islands (Agreement on the Conservation of Albatrosses and Petrels, 2010). The breeding season spans November through June, and they form mating pairs, laying one egg per season, although they may skip a year between breeding episodes (Tickell, 2000; Warham, 1990). Both males and females share parental duties and alternate foraging excursions during the first half of breeding. During the incubation period, foraging trips last one to three weeks, but after the chick hatches, trips become shorter and more frequent, lasting one to three days (Fernández et al., 2001; Hyrenbach et al., 2002; Kappes et al., 2015, 2010). These short trips reduce the accessible foraging area (Antolos et al., 2017), leaving the birds vulnerable to reproductive failure if geographic shifts in the foraging habitat places it outside the birds' foraging range (Kappes et al., 2015, 2010; Thorne et al., 2016, 2015). It is during the breeding season that the majority of black-footed albatross interactions occur with the Hawai'i-based longline fishery.

Black-footed albatrosses forage across the Pacific Ocean, and during the breeding season, they focus their foraging effort in the productive Subtropical Frontal Zone (STFZ) to the north of the Hawaiian Islands (Thorne et al., 2015). The STZF is a region of sharp changes in temperature and chlorophyll levels and is associated with the southern boundary of the westerlies. It is a surface convergent zone where the cold, productive waters of the subpolar gyre sink below the warm, low productivity waters of the subtropical gyre (Howell et al., 2012; Roden, 1980; Seki et al., 2002). Towards the southern border of the convergent zone lies the Transition Zone Chlorophyll Front (TZCF), a biological front defined by the 0.2 mg/m^3 chlorophyll line (Polovina et al., 2001), which has long been identified as important foraging habitat for marine birds and turtles (Polovina et al., 2017, 2001; Thorne et al., 2015). The latitudinal location of the TZCF varies throughout the year, with its southernmost extent – near 30°N – occurring during winter (Jan–Mar; Polovina et al., 2001). It extends further south during El Niño periods and further north during La Niña periods (Bograd et al., 2004). This southward displacement during El Niño periods is caused by a strong Aleutian low pressure system that extends the westerlies southward, which in turn pushes the subtropical convergence zone and TCZF to the south through Ekman transport (Bograd et al., 2004; Howell et al., 2012). This productive zone is brought closer to the black-footed albatross nesting colonies and overlaps with the Hawai'i-based longline fishing grounds.

What caused the recent increase in black-footed albatross interactions is unknown, but possible factors such as changes in fishing ground location or fishing season, changes in oceanography, or increases in the size of the black-footed albatross population have been suggested as potential drivers. While seabird interactions occur in both the shallow-set and deep-set fisheries, only 21% of shallow-set interactions are fatal compared to > 95% in the deep-set fishery (Pacific Islands Regional Office, 2018a). Because of the higher mortality rate and the larger size of the deep-set fishery (53,013,297 and 1,027,013 hooks set in 2017 in the deep-set and shallow-set fishery, respectively; Pacific Islands Fisheries Science Center (U.S.) Fisheries Research and Monitoring Division, 2018), we focus on the deep-set component of the fleet only. In this study, we investigate recent increases in black-footed albatross interactions with the Hawai'i-based longline fishing fleet. We identify potential drivers behind the increase and determine whether it is due to changes in fleet behavior or changes in environmental variables. Specifically, we build generalized linear models (GLMs) which allow us to predict black-footed albatross interactions based on fleet behavior alone or in combination with environmental variables. Finally, we use electronic tag data from breeding black-footed albatrosses to examine how their foraging areas can change interannually.

2. Methods

2.1. Observer data

Black-footed albatross sightings and interaction data were obtained from the Pacific Islands Regional Office Fisheries Observer Program (Pacific Islands Regional Office, 2018b). Observers cover approximately 20% of the deep-set fishing fleet, and they collect data on targeted and incidental catch for each set during a vessel trip. Five minutes after the start of each longline set observers conduct a 5-min seabird scans where they provide a best estimated number of seabirds of each species within ~140 m (150 yards) of the vessel ["sightings data"] (Pacific Islands Regional Office, 2017). Each observer data record contains the date, time, longitude and latitude of each set, the count and species of fish caught, the number of each species of bird present during the scan, along with the count and species of seabirds hooked (interactions).

The observer dataset we used contains 20,649 set level records spanning 2006–2017. Seabird mitigation method regulations and observer reporting methods changed in 2006; therefore, we chose that year to start the time series to eliminate any confounding effects from changing mitigation effort and reporting effects. Longline fishing boats

are not required to use seabird mitigation methods when fishing below 23°N, thus occasional interactions with black-footed albatross south of 23°N were removed.

We calculated annual black-footed albatross catch rates by dividing the number of birds caught by the observed effort (number of hooks deployed on trips where observers were present).

It is important to note that observer data are fisheries-dependent data; however, they are not self-reported. They are recorded by an independent fisheries observer on board the vessel. Because albatross sightings are only counted in the first 5 min, there are instances where there are interactions without any recorded bird sightings as it may take more time for the birds to approach the fishing vessel.

2.2. Models

Black-footed albatross interactions are infrequent; therefore, we used sightings as a proxy to elucidate drivers of the recent increase in interactions. Pearson's product correlation between black-footed albatross interactions and sightings was calculated using the "cor.test" function in the "stats" packages in the statistical software R (R Core Team, 2017).

Observer data were used to construct GLMs for black-footed albatross sightings from January 2006 until December 2017, as a function of 13 fleet and environmental variables (Table 1). To investigate the effect of fleet behavior on black-footed albatross sightings, the GLM used independent variables of month (as a factor), latitude, and longitude, allowing the latitude and longitude to interact. GLMs using environmental independent variables along with fleet behavior (month, latitude, and longitude) were constructed to evaluate the effects of environmental and climate variables. Because the data were overdispersed, we used a negative binomial GLM with a log link function, using the "glm.nb" function in the "MASS" package (Venables and Ripley, 2002) for R (R Core Team, 2017). All GLM's were constructed using a forward stepwise selection method where we started with a model containing no predictors, adding predictors to the model one at a time. At each step, the predictor variable generating the model with lowest AIC was chosen.

2.3. Fleet dynamics

The Hawai'i-based deep-set longline fishery shifts in space and time; different geographic areas are fished during different parts of the year and effort is distributed unevenly throughout the year (Woodworth-Jefcoats et al., 2018). To determine if the recent increase in interactions and sightings can be explained by changes in behavior of the fishing fleet, we included the month that the fishing occurred – to capture the seasonality of the fishery – and the latitude and longitude for the start of the set – to capture the horizontal movement of the fishery. These data were obtained from the observer dataset and were on a set level resolution spanning 2006 through 2017. We only included sightings north of 23°N where seabird mitigation measures are in place.

2.4. Regional environmental drivers and broad scale climate factors

Environmental data were accessed through OceanWatch (oceanwatch.pifsc.noaa.gov) and CoastWatch (coastwatch.pfeg.noaa.gov) and are monthly composites from January 2006 through December 2017, averaged over the core interaction area spanning 23–30°N and 150–165°W. We chose to average over this area because the bulk of fishing effort north of 23°N occurs there and the majority of black-footed albatross interactions take place within this core area (Fig. 1). This core interaction region lies between the climatological northern boundary of the trade winds and the southern boundary of the westerlies. There is considerable interannual and decadal variation in the position of this boundary. During El Niño and positive phases of the Pacific Decadal Oscillation (PDO), the Aleutian Low expands and the westerlies shift southward into the fishing grounds, while during La Niña and negative phases of the PDO, trade winds expand northward through the fishing grounds. The fishing grounds also lie in a north-south gradient of nutrients and productivity with high nutrients and productivity to the north which expands southward due to Ekman transport as westerlies expand southward. Thus, we selected regional environmental variables to capture the variation in the westerlies vs trades or proxies of surface productivity in this core interaction area (Table 1).

Monthly u- and v-velocities were not available for Jan–Feb 2014. Instead, monthly averages of 14-day composite data were used. Monthly composites data for wind stress curl were missing for Jan 2014, and a monthly average of the 14-day composite data was used in its stead. Additionally, wind stress curl data were anomalous (several orders of magnitude higher than other months) for August 2013. With no replacement wind curl data available and because sightings were low during that month, all records for August 2013 were removed. Wind speed was calculated from the monthly u- and v-velocities.

The Multivariate ENSO Index (MEI) is generated by NOAA's Earth Systems Research Laboratory and available from their website

Table 1
Environmental and biological variables used as predictors for the stepwise forward generalized linear models constructed to predict the black-footed albatross sightings.

Variable	Interpretation	Data Source	Temporal resolution
Month	Seasonality	Observer collected data	Per set
Longitude	Movement of fishery	Observer collected data	Set
Latitude	Movement of fishery	Observer collected data	Set
Hooks set	Effort	Observer collected data	Set
Number of nests	BFAL Population size	U.S. Fish and Wildlife	Nesting year (Nov–Jun)
Zonal wind velocity (u-vel)	Wind direction	QuickSCAT 2006–2009 METOP-A 2009–2017	Monthly composite
Meridional wind velocity (v-vel)	Wind direction	QuickSCAT 2006–2009 METOP-A 2009–2017	Monthly composite
Wind stress curl	Front strength	QuickSCAT 2006–2009 METOP-A 2009–2017	Monthly composite
Wind speed	Wind strength	Calculated from u- and v- velocities above	Monthly composite
Chlorophyll a	Productivity	Aqua MODIS	Monthly composite
Mean sea surface temperature (SST)	Water mass	AVHRR Pathfinder v.4.1 & AVHRR GAC 2006–2012 GOES/POES 2013–2017	Monthly composite
SST Standard deviation	Front strength	AVHRR Pathfinder v.4.1 & AVHRR GAC 2006–2012 GOES/POES 2013–2017	Monthly composite
Pacific Decadal Oscillation (PDO)	Broad scale variability	http://research.jisao.washington.edu/pdo/PDO.latest.txt	Monthly
Multivariate ENSO Index (MEI)	Broad scale variability	https://www.esrl.noaa.gov/psd/enso/mei/table.html	Bimonthly

(Table 1). The PDO index is generated at the University of Washington Institute for the Study of the Atmosphere and Ocean and was downloaded from their website (Table 1).

Black-footed albatross nesting data for Midway Atoll were obtained from U. S. Fish and Wildlife Service Marine National Monuments of the Pacific. Nest counts are used as a proxy for population size in oceanic seabirds, and we used counts from Midway Atoll because no recent data were available for Tern Island or other nesting sites in the Northwestern Hawaiian Islands. Nest counts were used to determine if a relationship exists between increased fisheries interactions and increased breeding population size of black-footed albatross. While we do not know if changes to Midway Atoll nest counts are representative of changes in the black-footed albatross population as a whole, Midway supports ~39% of the breeding pairs (Agreement on the Conservation of Albatrosses and Petrels, 2010) and is the only location with a time series spanning 2006–2017.

2.5. Model evaluation

To evaluate the performance of the GLMs, we predicted the black-footed albatross sightings using set location and mean monthly values of the biological and environmental variables averaged over the core interaction area described above. We then calculated the Pearson's product correlation between the observed and predicted black-footed albatross sightings. Additionally, the Akaike information criterion (AIC) was used as an alternative way to rank candidate model fit.

Additionally, we performed a two-fold cross validation to evaluate the stability and performance of the model predictions. There was no change in model performance, so all results presented are for models build on the full dataset.

2.6. Black-footed albatross flight tracks

Observer data built a rich dataset of black-footed albatross distributions. But because this dataset is fishery-dependent, it has some drawbacks. Observer data are not able to provide information on black-footed albatross locations outside the fishing grounds, and spatial movement of the fleet will influence the spatial patterns of black-footed albatross sightings. To address these shortcomings of observer data, we used GPS location data for 48 individual black-footed albatrosses tracked from Tern Island, French Frigate Shoals (Fig. 1) between 2006 and 2012. The tracking data from Tern Island were collated from (Conners et al., 2015). Analysis methods of the GPS tracking data are described in (Conners et al., 2015) and modified in (Shaffer et al., 2017). In this study we focused on core habitat use rather than individual behaviors, so we allowed multiple trips made by the same bird. Not all tracks had the same logging time interval (10 s–10 min); therefore, we subsampled the data to include only one location each hour. The duration black-footed albatrosses spent traveling/foraging across latitudes was calculated as cumulative frequency of hourly locations from south to north for positive (PDO index $>$ 0) and negative (PDO index $<$ 0) PDO phases.

3. Results

Black-footed albatross interaction rates over the time period were highest in 2015 through 2017, with the sharpest increase in 2015 (Fig. 2). The interactions during 2015 were atypical, with the majority of interactions occurring in June instead of during the first quarter, and two boats were responsible for hooking 40% of the birds. Similarly, black-footed albatross sightings increased during 2015–2017 compared with the previous nine years (Fig. 2). Sightings increased most sharply in 2016 while interactions increased most sharply in 2015, a further indication that the 2015 interactions were atypical.

Black-footed albatross interactions were infrequent, with only 410 sets (1.95%) reporting interactions from 2006 through 2017, and with a total of 470 black-footed albatross interactions north of 23°N. These interactions were insufficient to generate a significant generalized linear model (GLM), nor were we able to generate a stable random forest model due to the strong zero-inflation in the data and the low number of interactions. However, there was a positive correlation ($R^2 = 0.58$, $p < 0.001$) between black-footed albatross interactions and sightings (Fig. 3), allowing us to use sightings as a proxy for interactions.

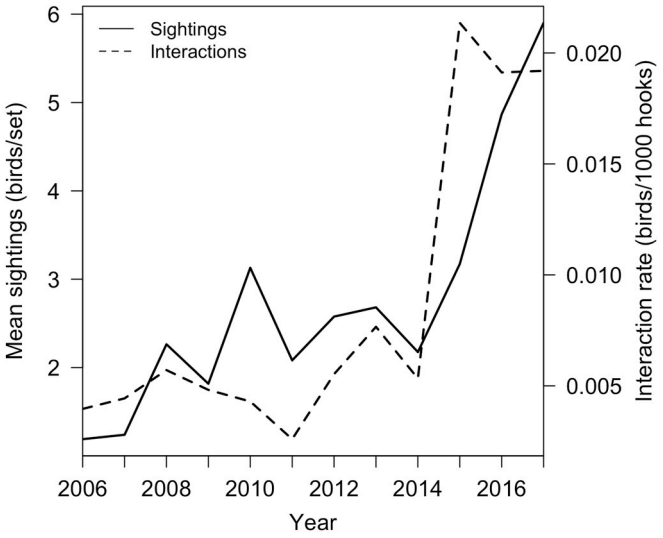

Fig. 2. Annual black-footed albatross interaction rates (number of birds per 1000 hooks set; dashed line) and mean black-footed albatross sightings (per set; solid line) in the Hawai'i-based deep-set longline fishery north of 23°N from January 2006 through December 2017.

3.1. Generalized linear models (GLMs)

3.1.1. Fleet behavior

Fleet behavior, defined here as the geographic location and month of sighting, was significant in explaining black-footed albatross sightings. Sightings were highest during the breeding season (Dec–Apr) and increased to the north and to the west (Fig. 4a–c). The correlation between observed sightings and predicted sightings using the fleet behavior GLM was strong ($r = 0.79$, $p < 0.001$, Fig. 5a). Our model captures

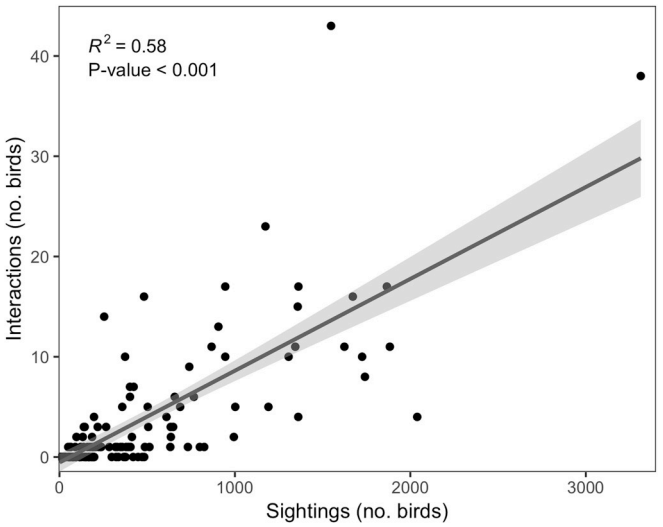

Fig. 3. Linear correlation between total monthly black-footed albatross sightings and interactions north of 23°N latitude from January 2006 until December 2017. The gray shading represents ± two standard errors.

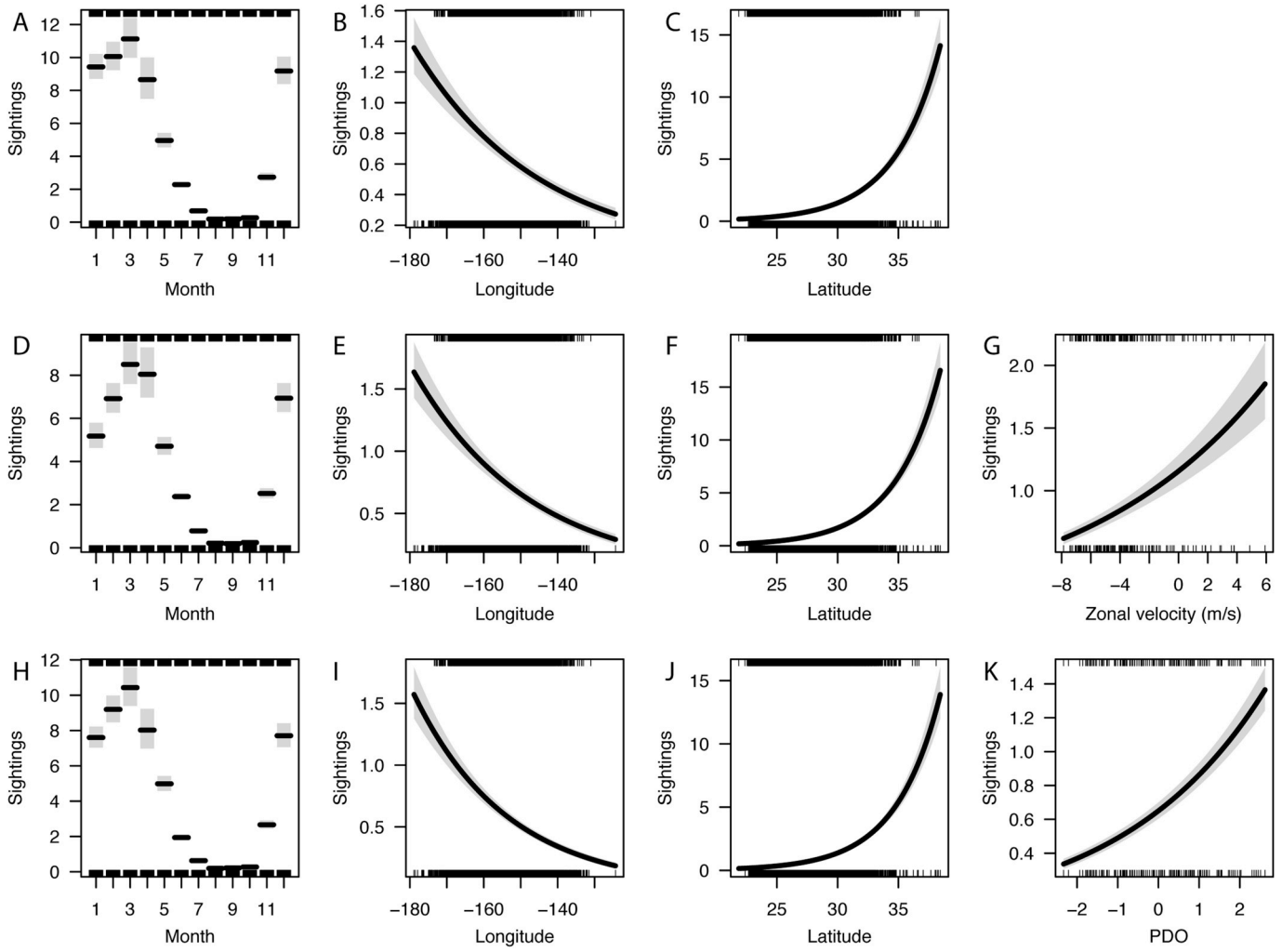

Fig. 4. Linear predictors for three candidate general linear models (GLMs) evaluating sightings as a function of (1) fleet behavior [A-C], (2) regional oceanography [D-G], and (3) larger scale climate variability [H-K]. All models had the same linear predictor pattern for month, latitude, and longitude, so only the fleet behavior model predictors are shown. For all three models, sightings are highest in March and lowest in the third quarter [A,D,H], they increase to the west [B,E,I] and north [C,F,J], and with an increase in zonal (u) wind velocities [G] and during positive PDO phases [K]. The linear predictors are scaled to the original response, and the shaded area shows ± two standard error. Conditions used for plots are latitude 27.13, longitude −155.5, month 7, zonal velocity −4.9, and PDO -0.11.

the seasonality of the sightings but underestimates the sightings for years 2015 and 2016 – two years with unusually high black-footed albatross interactions.

Effort was not included in the fleet behavior model since bird sightings are collected 5 min after the start of the set and the number of hooks deployed during the set do not influence the sightings data. For completeness we evaluated effort as a driver but did not include it in the final fleet behavior model. The number of hooks per set increased by 22.5% over the span of the 12-year time series, but the increase was gradual and did not explain the 2015 increase in black-footed albatross sightings (Fig. S2).

3.2. Regional environmental drivers

Zonal wind velocity (u-velocity) was the best predictor of sightings out of the candidate models that include environmental variables (Table 2). As with the fleet dynamic model, the u-velocity model predicted an increase in sightings to the north and west, with a peak in March (Fig. 4d–f). Predicted sightings also increased with intensifying westerly winds and were lowest during strong trade wind conditions (negative u-velocities) (Fig. 4g). Observed and predicted sightings were strongly correlated ($r = 0.87$, $p < 0.001$), and predictions for sightings during 2016 improved compared to the fleet behavior model (Fig. 5a and b). However, the predictions were still underestimated in 2015.

The standard deviation of Sea Surface Temperature (SST sd) was the second-best predictor of sightings out of the regional environmental drivers (Table 2), and sightings increased with increasing SST sd values (Fig. S1). The standard deviation of SST can be used as an indicator of front strength with a higher value representing a stronger temperature front.

The remaining regional environmental drivers, in order of predictor strength, were SST mean, chlorophyll a, meridional wind velocity, and wind stress curl. All drivers showed the same spatial pattern with sightings increasing to the north and west, and all but mean SST peaked in March. Sightings increased with increasing chlorophyll a and wind stress curl, but decreased with increasing meridional winds and mean SST (Fig. S1). Wind speed was the only environmental variable that was not a significant predictor of sightings.

3.3. Broad scale climate factors

Focusing on larger scale climate variability, the GLM with Pacific Decadal Oscillation (PDO) was the best predictor of black-footed albatross sightings. Consistent with the other candidate models, sightings increased during the breeding season and to the north and west (Fig. 4h–j). Sightings also increased with increasing PDO; sightings

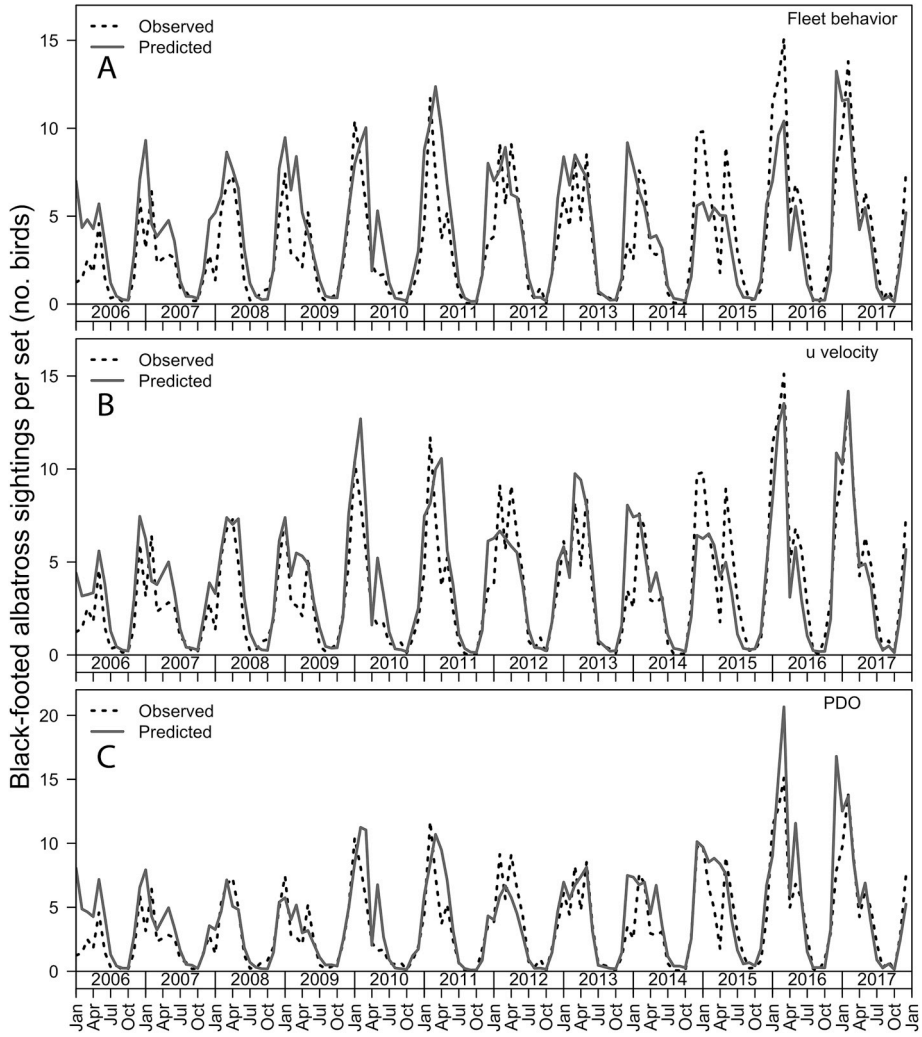

Fig. 5. Observed (dotted) and generalized linear model predicted (solid) mean monthly black-footed albatross sightings per set for 2006 through 2017 for fleet behavior (top), zonal wind velocity (middle), and Pacific Decadal Oscillation (PDO) (bottom). Zonal wind velocity acts on a regional scale while PDO on a sub-basin scale. The annual increase in sightings coincides with the albatross breading season.

Table 2
Table showing GLM performance of twelve models using oceanographic data and fleet behavior. The AIC from the GLM and the Pearson's product correlation coefficient (r) between the observed and model predicted black-footed albatross sightings are listed. All models and variables were highly significant with $p < 1 \times 10^{-5}$ except for wind speed which was non-significant.

Variable	r	AIC
Fleet behavior + Wind u-velocity	0.868	70531
Fleet behavior + PDO	0.854	69977
Fleet behavior + SST st. dev.	0.837	70559
Fleet behavior + MEI	0.834	70357
Fleet behavior + Effort	0.825	70498
Fleet behavior + SST mean	0.807	70630
Fleet behavior + Chlorophyll a	0.795	70413
Fleet behavior + Wind v-velocity	0.79	70634
Fleet behavior (month, latitude, longitude) only	0.79	70691
Fleet behavior + Nests	0.768	70558
Fleet behavior + Wind stress curl	0.76	70648
Fleet behavior + Wind speed	*0.8*	*70691*

were higher during positive PDO and lower during the negative PDO phases (Fig. 4k). Our model captured the 2015 sightings but overestimated sightings for 2016 (Fig. 5c).

The GLM predicted sightings based on fleet behavior and Multivariate ENSO Index (MEI) had the fourth highest correlation with observed sightings overall (Table 2, Fig. S1). Sightings increased with increasing MEI, indicating that they were higher during El Niño years (positive MEI) and lower during La Niña years (negative MEI). Overall correlation was high, but the model underestimated the 2015 and overestimated the 2016 sightings (Fig. S2).

3.4. Nest counts

The increase in sightings in 2015–2017 was likely not due to an increase in albatross nesting population size. Of the candidate GLMs, predictions from the model including nest counts had the second lowest correlation with observed sightings (Table 2). While there was a slight increase in sightings with increased nest counts (Fig. S1), nest counts overall did not vary substantially over the duration of the time series (25,392 ± 572 se counts). The GLM underestimated the 2015–2016 increase in sightings and only slightly improved the fit of the fleet behavior model (Fig. S2, Table 2).

3.5. Black-footed albatross habitat use

There were 137 individual black-footed albatross tracks recorded between November and March during six nesting years between 2006 and 2012 (Table 3).

Because the PDO improved the fit in the sightings GLM, the tracking

Table 3
Tracking information for black-footed albatross originating at Tern Island during six breeding years. Positive PDO phase was defined as PDO index > 0 and negative PDO as PDO index < 0.

No. tracks	Month	Year	PDO phase
6	Jan–Feb	2006	Positive
25	Jan–Mar	2007	Negative
29	Dec–Feb	2008/2009	Negative
32	Dec–Mar	2009/2010	Positive
9	Dec–Jan	2010/2011	Negative
36	Dec–Feb	2011/2012	Negative

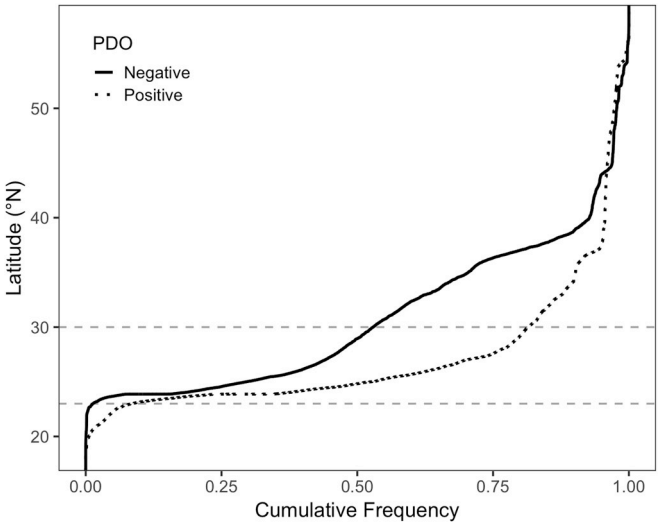

Fig. 6. Cumulative frequency of black-footed albatross track distributions with latitude for positive (dotted) and negative (solid) Pacific Decadal Oscillation years. All birds were tagged and nesting on Tern Island in the Northwestern Hawaiian Islands, and all tracks were recorded between November and March. There were 38 tracks during the positive PDO years (2005/2006 and 2009/2010) and 99 tracks during negative PDO years (2006/2007, 2008/2009, 2010/2011 and 2011/2012). Gray, dashed lines mark the high interaction zone 23–30°N.

data were grouped by years defined by positive and negative PDO to examine whether their spatial foraging patterns changed between the two regimes. The birds spent more time south of 30°N during positive PDO years (81%) compared to negative PDO years (57%)(Fig. 6).

4. Discussion

We found that the increase in black-footed albatross sightings and corresponding rise in interactions were not explained by fleet behavior alone. They were best explained by a combination of fleet behavior and regional environmental variables: specifically, strong westerly winds and large changes in sea surface temperature (SST) – the result of a positive Pacific Decadal Oscillation (PDO) phase. With a positive phase PDO, winds in the core interaction area (23–30°N and 150–165°W) are predominately westerlies rather than the trades that dominate during a negative phase PDO (Mantua and Hare, 2002; Newman et al., 2016). This shift in wind direction may have two impacts. Firstly, westerlies drive colder nutrient-rich and productive surface waters southward into the core interaction area, potentially improving foraging habitat for black-footed albatross and hence increasing the density of black-footed albatrosses within the fishing grounds. Secondly, black-footed albatrosses travel east and northeast from their nesting sites, west of the fishing grounds to reach their foraging habitat (Conners et al., 2015; Fernández et al., 2001; Hyrenbach et al., 2002; Thorne et al., 2016). Under trade wind conditions, albatrosses appear to head northward to reach westerly winds that carry them eastward, while under westerly wind conditions, birds can head eastward without first going northward and are more likely to enter into the fishing grounds that lie south of 30°N latitude (Fig. 1).

The discrepancy between interactions and sightings in 2015 suggests that it was an anomalous year, and for that year drivers behind the increased interactions did not affect the number of sightings. This difference can be explained by irregular interactions in 2015, when 40% of black-footed albatross interactions occur with just two fishing vessels. Observer records show that proper seabird mitigation methods were in place and the discrepancy may be due to albatrosses attending the vessels after the observer scan was finished or after the occurrence of an unusually aggressively feeding flock of birds for example. The discrepancy between sightings and interactions further explains why most of our candidate models had difficulty predicting the 2015 interactions accurately; and why, if they were successful, greatly overestimated the 2016 interactions.

4.1. Fleet behavior

The GLM based solely on fleet behavior did not fully explain the increased black-footed albatross sightings in 2015–2017. While the Hawai'i-based deep-set longline fishing fleet has shifted its footprint from south and west of the main Hawaiian Islands towards the north and east over the past 20 years, this change has taken place predominantly during the third quarter of the year (Woodworth-Jefcoats et al., 2018) – after black-footed albatross chicks are fledged and adult foraging range is no longer constrained by breeding duties (Gutowsky et al., 2014). Accounting for the geographic location of the fishing fleet in addition to the seasonality of the fishery, we were successful in predicting the annual cycle of black-footed albatross sightings, but not the recent peak in sightings.

Effort, or the number of hooks deployed per set, has gradually increased over time, and fishing effort cannot explain the sudden increase in sightings when added to the fleet behavior model. While number of hooks set may influence black-footed albatross interactions, they are unlikely to influence sightings, as birds are counted 5 min after the start of the set and are not influenced by the length of a set or the number of hooks deployed.

4.2. Regional environmental drivers

Changes in wind direction from trade winds to westerlies best explained the increase in black-footed albatross sightings. When foraging, black-footed albatross seek out and follow physical oceanographic features (e.g., SST and/or chlorophyll fronts) that change locations from year to year, rather than frequent a static feeding ground (Hyrenbach et al., 2002; Kappes et al., 2010; Žydelis et al., 2011). These frontal systems (i.e., STFZ) are located north of the breeding grounds and are identified by rapid changes in sea surface temperature (SST) and/or productivity. The deep-set longline fishing fleet targets different, sub-surface productivity areas further to the south that are more stationary from year to year. Additionally, the northward movement of the longline fishing fleet is limited past 35°N, and the deep-set longline fishery consistently expend the bulk of their effort south of 30°N latitude, particularly during the first 6 months of the year (Woodworth-Jefcoats et al., 2018). We determined that when winds shift from trades to westerlies and there is a subsequent strengthening of the temperature front (standard deviation of SST) and increased chlorophyll a concentration in the high interactions area (23–30°N, 150–165°W), more black-footed albatrosses attend vessels, suggesting there is an increased overlap between the black-footed albatross foraging grounds and the more stationary longline fishing grounds.

The increase in sightings of black-footed albatrosses during westerly winds may also be due to flight energetics. For energy efficient soaring flight, albatrosses require strong wind regimes and avoid headwinds

(Suryan et al., 2008; Weimerskirch et al., 2012). They use westerly winds – and avoid trade winds – to transit east to their foraging grounds (Thorne et al., 2016, 2015). This is supported by both tracking and model data: albatrosses spend more time south of 30°N during positive PDO phases, and sightings increase during strong westerly winds but not during strong trade winds.

Albatrosses and other seabirds are known to scavenge off fishing vessels and fisheries discards can be an important food source during chick rearing (Bugoni et al., 2010; Granadeiro et al., 2011; James and Stahl, 2000). Additionally, black-footed albatrosses may opportunistically scavenge on discarded bait and offal when they encounter fishing vessels, without intentionally seeking the vessel out. Researchers have suggested that an increase in interactions and sightings of albatrosses in Hawai'i is caused by an increase in scavenging from vessels by the birds when productivity is low during El Niño conditions (Gilman et al., 2016). We see no evidence of this, as we would expect sightings to be higher when productivity is lower in the core interaction area, the opposite of our results. However, during El Niño events the equatorial Pacific has low productivity, but the waters around Hawai'i show the opposite pattern with cooler waters and increased productivity (see section 4.3). Whether the increased sightings are due to increased overlap between foraging and fishing grounds, or if birds are merely transiting through the fishing grounds instead of around them and opportunistically scavenge on bait and discard from longline vessels, or both, remains unknown but is an area of active research. By using biologgers capable of detecting ship radar scientists are getting closer to identifying seabird behavior in relation to vessels (Weimerskirch et al., 2018, Shaffer unpublished data)

4.3. Broad scale climate factors

During positive PDO conditions, a strong Aleutian low-pressure system to the north of Hawai'i generates strong westerly winds which in turn displaces cold, nutrient rich waters southward towards the Hawaiian Islands through Ekman transport. While black-footed albatross foraging behavior likely responds to regional environmental variables, such as wind direction and ocean productivity, the broad scale climate processes (e.g., PDO and ENSO) that drive these regional changes generate the best fit models for predicting sightings. These findings are consistent with previous studies linking albatross sightings and interactions to the MEI (Gilman et al., 2016) and the PDO (Michael et al., 2016) and indicate that black-footed albatrosses target the subtropical frontal systems to the north of the breeding colonies and follow them as they shift from year to year.

The MEI candidate model was the second best model based on AIC value for predicting sightings in the Hawai'i longline fleet. El Niño – Southern Oscillation (ENSO) influences ocean conditions in the North Pacific through the "atmospheric bridge" and drives PDO on interannual time scales (Alexander et al., 2002; Schneider and Cornuelle, 2005), making it logical that ENSO would be a good overall predictor of black-footed albatross sightings. However, the MEI candidate model does an inferior job at recreating the 2015–2017 increase in sightings compared with models using wind, PDO, and variations in sea surface temperature. PDO better captures the local atmospheric and oceanographic changes that guide black-footed albatross foraging.

PDO has a stronger response in north Pacific mid-latitudes compared with other broad scale climate factors such as ENSO and the North Pacific Gyre Oscillation (Di Lorenzo et al., 2010; Mantua and Hare, 2002; Newman et al., 2016). The short-term PDO patterns are forced by ENSO as well as the Aleutian low (Schneider and Cornuelle, 2005), resulting in periods with positive PDO phases associated with more frequent El Niño events, and negative PDO phases with more frequent La Niña events (Verdon and Franks, 2006). The PDO phase shifted from negative to positive in 2014, and 2014–2017 were the first years in our timeseries with concurrent positive PDO and El Niño conditions. The enhancement of the positive PDO patterns seen during this time likely contributes to the abrupt increase in sightings and interactions in 2015.

The PDO and MEI are less variable than winds and easier to predict for a given breeding year. However, with a periodicity of years and decades for MEI and PDO, respectively, the observer data timeseries may be too short to determine if positive PDO and El Niño (positive MEI conditions) conditions are appropriate predictors of increased sightings and interactions. This relationship should be evaluated in the future when a longer black-footed albatross interactions timeseries is available.

While foraging efficiency and reproductive success may increase during positive PDO and El Niño conditions (Thorne et al., 2016; Weimerskirch et al., 2012), our results indicate that this positive effect may be offset by an increase in adult mortality from increased fisheries interactions. A recent black-footed albatross population study suggests that the current mortality rates caused by fisheries interactions are higher than what is required to sustain and grow the population and urges further bycatch reduction (Bakker et al., 2018). While bycatch reduction in the Hawai'i-based longline fishery has been successful in the past (Gilman et al., 2016), albatross interactions may be underreported by as much as 50% (Brothers et al., 2010), suggesting that further methods for lowering black-footed albatross interactions are needed. Reevaluating additional mitigation methods, such as baiting hooks under water (Gilman et al., 2007, 2003; Robertson et al., 2018) and bird-scaring lines (Boggs, 2001; Melvin et al., 2014), is warranted.

4.4. Black-footed albatross distributions and habitat use

The observer data provide an opportunity to identify potential drivers behind patterns in black-footed albatross sightings and fisheries interactions. However, it is important to keep in mind that observer data are fishery-dependent, and underlying drivers of black-footed albatross distributions may not be encountered by the fishing fleet or recorded by the observer. Fisheries-independent data, such as bird tracking data, however, allows us to form a more complete picture of black-footed albatross distributions in space and time (Fernández et al., 2001; Hyrenbach et al., 2002; Kappes et al., 2015, 2010). In the present study, GPS tracking data showed that black-footed albatrosses spend 42% more time south of 30°N during positive PDO phase years compared to negative PDO phase years. Hence, the tracking data support our model findings, lending further strength to the idea that large scale climate variability affects black-footed albatross foraging patterns (Thorne et al., 2016, 2015, this study), and in extension, interactions.

5. Conclusions

In the present study, we identified potential drivers behind the recent increase in black-footed albatross interactions and sightings in the Hawai'i-based deep-set longline fishery. While we were not successful in calculating specific drivers behind black-footed albatross interactions due to scarcity of data, we were able to show that interactions and sightings are correlated. We found that both fleet dynamics and environmental variables linked to PDO explain much of the variation in black-footed albatross sightings around longline vessels. Sightings are primarily driven by PDO patterns, and the increase in sightings in 2015–2017 is best explained by a southern shift of the westerlies and an increase in surface productivity in the fishing grounds, resulting in greater overlap between the black-footed albatross foraging grounds and the deep-set longline fishing grounds. These findings were supported by black-footed albatross track data which showed that the birds spend substantially more time in the deep-set longline fishing grounds south of 30°N during years with positive phase PDO than during years with negative phase PDO. Because of these underlying decadal scale drivers (i.e., PDO), the high levels of sightings and interactions may persist for many years rather than being a short episodic event.

Interest statement

Declarations of interest: none.

Acknowledgements

The authors wish to thank the scientific observers of the Pacific Islands Region for their collection of longline fisheries data; John Peschon and Eric Forney for help accessing and understanding the nuances of the data; Melinda Conners and Morgan Gilmour for assistance in the field to collect the GPS tracking data; Felipe Carvalho, Michelle Sculley, and Brian Stock for invaluable help with data analysis; Beth Flint and Allie Hunter for sharing nesting census data; OceanWatch and CoastWatch for remotely sensed data; and David Hyrenbach, Sara Ellgen, Tamara Russell, Asuka Ishizaki, Phoebe Woodworth-Jefcoats, Melanie Abecassis, and the 2017 WPRFMC Albatross workshop for fruitful discussions that greatly improved our understanding of black-footed albatross ecology. The albatross tracking work was supported by cooperative agreements between USFWS, Division of Migratory Birds and S.A. Shaffer.

Appendix A. Supplementary data

Supplementary data to this article can be found online at https://doi.org/10.1016/j.dsr2.2019.06.013.

References

Agreement on the Conservation of Albatrosses and Petrels, 2010. Species Assessments: Black-Footed Albatross *Phoebastria nigripes*.
Alexander, M.A., Bladé, I., Newman, M., Lanzante, J.R., Lau, N.-C., Scott, J.D., 2002. The atmospheric bridge: the influence of ENSO teleconnections on air–sea interaction over the global oceans. J. Clim. 15, 2205–2231.
Antolos, M., Shaffer, S.A., Weimerskirch, H., Tremblay, Y., Costa, D.P., 2017. Foraging behavior and energetics of albatrosses in contrasting breeding environments. Front. Mar. Sci. 4, 414.
Bakker, V.J., Finkelstein, M.E., Doak, D.F., VanderWerf, E.A., Young, L.C., Arata, J.A., Sievert, P.R., Vanderlip, C., 2018. The albatross of assessing and managing risk for long-lived pelagic seabirds. Biol. Conserv. 217, 83–95. https://doi.org/10.1016/j.biocon.2017.08.022.
Boggs, C.H., 2001. Deterring albatrosses from contacting baits during swordfish longline sets. Seab. Bycatch Trends, Roadblocks Solut. Univ. Alaska Sea Grant, Fairbanks, Alaska. AK-SG-01-01 79–94.
Bograd, S.J., Foley, D.G., Schwing, F.B., Wilson, C., Laurs, R.M., Polovina, J.J., Howell, E.A., Brainard, R.E., 2004. On the seasonal and interannual migrations of the transition zone chlorophyll front. Geophys. Res. Lett. 31.
Brothers, N., Duckworth, A.R., Safina, C., Gilman, E.L., 2010. Seabird bycatch in pelagic longline fisheries is grossly underestimated when using only haul data. PLoS One 5, e12491.
Bugoni, L., McGill, R.A.R., Furness, R.W., 2010. The importance of pelagic longline fishery discards for a seabird community determined through stable isotope analysis. J. Exp. Mar. Biol. Ecol. 391, 190–200.
Conners, M.G., Hazen, E.L., Costa, D.P., Shaffer, S.A., 2015. Shadowed by scale: subtle behavioral niche partitioning in two sympatric, tropical breeding albatross species. Mov Ecol 3, 28.
Di Lorenzo, E., Cobb, K.M., Furtado, J.C., Schneider, N., Anderson, B.T., Bracco, A., Alexander, M.A., Vimont, D.J., 2010. Central pacific El Niño and decadal climate change in the north Pacific Ocean. Nat. Geosci. 3, 1–4. https://doi.org/10.1038/ngeo984.
Fernández, P., Anderson, D.J., Sievert, P.R., Huyvaert, K.P., 2001. Foraging destinations of three low-latitude albatross (Phoebastria) species. J. Zool. 254, 391–404.
Gilman, E., Boggs, C., Brothers, N., 2003. Performance assessment of an underwater setting chute to mitigate seabird bycatch in the Hawaii pelagic longline tuna fishery. Ocean Coast Manag. 46, 985–1010.
Gilman, E., Brothers, N., Kobayashi, D.R., 2007. Comparison of three seabird bycatch avoidance methods in Hawaii-based pelagic longline fisheries. Fish. Sci. 73, 208–210.
Gilman, E., Chaloupka, M., Peschon, J., Ellgen, S., 2016. Risk factors for seabird bycatch in a pelagic longline tuna fishery. PLoS One 11, e0155477.
Gilman, E., Kobayashi, D., Chaloupka, M., 2008. Reducing seabird bycatch in the Hawaii longline tuna fishery. Endanger. Species Res. 5, 309–323.
Granadeiro, J.P., Phillips, R.A., Brickle, P., Catry, P., 2011. Albatrosses following fishing vessels: how badly hooked are they on an easy meal? PLoS One 6, e17467.
Gutowsky, S.E., Gutowsky, L.F.G., Jonsen, I.D., Leonard, M.L., Naughton, M.B., Romano, M.D., Shaffer, S.A., 2014. Daily activity budgets reveal a quasi-flightless stage during non-breeding in Hawaiian albatrosses. Mov. Ecol. 2, 23.
Howell, E.A., Bograd, S.J., Morishige, C., Seki, M.P., Polovina, J.J., 2012. On North Pacific circulation and associated marine debris concentration. Mar. Pollut. Bull. 65, 16–22.
Hyrenbach, K.D., Fernández, P., Anderson, D.J., 2002. Oceanographic habitats of two sympatric North Pacific albatrosses during the breeding season. Mar. Ecol. Prog. Ser. 233, 283–301.
James, G.D., Stahl, J., 2000. Diet of southern Buller's albatross (Diomedea bulleri bulleri) and the importance of fishery discards during chick rearing. N. Z. J. Mar. Freshw. Res. 34, 435–454.
Kappes, M.A., Shaffer, S.A., Tremblay, Y., Foley, D.G., Palacios, D.M., Bograd, S.J., Costa, D.P., 2015. Reproductive constraints influence habitat accessibility, segregation, and preference of sympatric albatross species. Mov Ecol 3, 34.
Kappes, M.A., Shaffer, S.A., Tremblay, Y., Foley, D.G., Palacios, D.M., Robinson, P.W., Bograd, S.J., Costa, D.P., 2010. Hawaiian albatrosses track interannual variability of marine habitats in the North Pacific. Prog. Oceanogr. 86, 246–260.
Lewison, R.L., Crowder, L.B., 2003. Estimating fishery bycatch and effects on a vulnerable seabird population. Ecol. Appl. 13, 743–753.
Mantua, N.J., Hare, S.R., 2002. The pacific decadal oscillation. J. Oceanogr. 58, 35–44.
Melvin, E.F., Guy, T.J., Read, L.B., 2014. Best practice seabird bycatch mitigation for pelagic longline fisheries targeting tuna and related species. Fish. Res. 149, 5–18.
Michael, P.E., Jahncke, J., Hyrenbach, K.D., 2016. Placing local aggregations in a {Larger-Scale} context: hierarchical modeling of {Black-Footed} albatross dispersion. PLoS One 11, e0153783.
National Oceanic and Atmospheric Administration (NOAA) National Marine Fisheries Service (NMFS), 2005. Fisheries off west coast states and in the western pacific; pelagic fisheries; additional measures to reduce the incidental catch of seabirds in the Hawaii pelagic longline fishery. Fed. Regist. Dly. J. United States 70, 75075–75080.
Newman, M., Alexander, M.A., Ault, T.R., Cobb, K.M., Deser, C., Di Lorenzo, E., Mantua, N.J., Miller, A.J., Minobe, S., Nakamura, H., Others, 2016. The Pacific decadal oscillation, revisited. J. Clim. 29, 4399–4427.
Pacific Islands Fisheries Science Center (U.S.) Fisheries Research and Monitoring Division, 2018. The Hawaii Limited Access Longline Logbook Summary Report January to December 2017. Honolulu, HI, USA.
Pacific Islands Regional Office, 2018a. Seabird Interactions and Mitigation Efforts in Hawaii Longline Fisheries - 2016 Annual Report.
Pacific Islands Regional Office, 2018b. Longline Observer Data System. https://inport.nmfs.noaa.gov/inport/item/9027.
Pacific Islands Regional Office, 2017. Hawaii Longline Observer Program Field Manual Version LM 17.02.
Polovina, J.J., Howell, E.A., Kobayashi, D.R., Seki, M.P., 2017. The transition zone chlorophyll front updated: advances from a decade of research. Prog. Oceanogr. 150, 79–85.
Polovina, J.J., Howell, E.A., Kobayashi, D.R., Seki, M.P., 2001. The transition zone chlorophyll front, a dynamic global feature defining migration and forage habitat for marine resources. Prog. Oceanogr. 49, 469–483.
R Core Team, 2017. R: A Language and Environment for Statistical Computing.
Robertson, G., Ashworth, P., Ashworth, P., Carlyle, I., Jiménez, S., Forselledo, R., Domingo, A., Candy, S.G., 2018. Setting baited hooks by stealth (underwater) can prevent the incidental mortality of albatrosses and petrels in pelagic longline fisheries. Biol. Conserv. 225, 134–143. https://doi.org/10.1016/j.biocon.2018.06.026.
Roden, G.I., 1980. On the subtropical frontal zone north of Hawaii during winter. J. Phys. Oceanogr. 10, 342–362.
Schneider, N., Cornuelle, B.D., 2005. The forcing of the pacific decadal oscillation. J. Clim. 18, 4355–4373.
Seki, M.P., Polovina, J.J., Kobayashi, D.R., Bidigare, R.R., Mitchum, G.T., 2002. An oceanographic characterization of swordfish (Xiphias gladius) longline fishing grounds in the springtime subtropical North Pacific. Fish. Oceanogr. 11, 251–266.
Shaffer, S.A., Cockerham, S., Warzybok, P., Bradley, R.W., Jahncke, J., Clatterbuck, C.A., Lucia, M., Jelincic, J.A., Cassell, A.L., Kelsey, E.C., Adams, J., 2017. Population-level plasticity in foraging behavior of western gulls (Larus occidentalis). Mov Ecol 5, 27.
Suryan, R.M., Anderson, D.J., Shaffer, S.A., Roby, D.D., Tremblay, Y., Costa, D.P., Sievert, P.R., Sato, F., Ozaki, K., Balogh, G.R., Nakamura, N., 2008. Wind, waves, and wing loading: morphological specialization may limit range expansion of endangered albatrosses. PLoS One 3, e4016. https://doi.org/10.1371/journal.pone.0004016.
Thorne, L.H., Conners, M.G., Hazen, E.L., Bograd, S.J., Antolos, M., Costa, D.P., Shaffer, S.A., 2016. Effects of El nino-driven changes in wind patterns on north Pacific albatrosses. J. R. Soc. Interface 13, 20160196.
Thorne, L.H., Hazen, E.L., Bograd, S.J., Foley, D.G., Conners, M.G., Kappes, M.A., Kim, H.M., Costa, D.P., Tremblay, Y., Shaffer, S.A., 2015. Foraging behavior links climate variability and reproduction in North Pacific albatrosses. Mov Ecol 3, 27.
Tickell, W.L.N., 2000. Albatrosses. Yale University Press.
Tuck, G.N., Polacheck, T., Croxall, J.P., Weimerskirch, H., 2001. Modelling the impact of fishery by-catches on albatross populations. J. Appl. Ecol. 38, 1182–1196.
Venables, W.N., Ripley, B.D., 2002. Modern Applied Statistics with S, Fourth. Springer, New York.
Verdon, D.C., Franks, S.W., 2006. Long-term behaviour of ENSO: interactions with the PDO over the past 400 years inferred from paleoclimate records. Geophys. Res. Lett. 33.
Warham, J., 1990. The Petrels: Their Ecology and Breeding Systems. A&C Black.
Weimerskirch, H., Filippi, D.P., Collet, J., Waugh, S.M., Patrick, S.C., 2018. Use of radar detectors to track attendance of albatrosses at fishing vessels. Conserv. Biol. 32, 240–245.
Weimerskirch, H., Louzao, M., de Grissac, S., Delord, K., 2012. Changes in wind pattern alter albatross distribution and life-history traits. Science (80-.) 335, 211–214.
Woodworth-Jefcoats, P.A., Polovina, J.J., Drazen, J.C., 2018. Synergy Among Oceanographic Variability, Fishery Expansion, and Longline Catch Composition in the Central North Pacific Ocean. FB 116. pp. 228–239.
Žydelis, R., Lewison, R.L., Shaffer, S.A., Moore, J.E., Boustany, A.M., Roberts, J.J., Sims, M., Dunn, D.C., Best, B.D., Tremblay, Y., Kappes, M.A., Halpin, P.N., Costa, D.P., Crowder, L.B., 2011. Dynamic habitat models: using telemetry data to project fisheries bycatch. Proc. R. Soc. Biol. Sci. 278, 3191–3200.